Applied Mathematical Modelling 39 (2015) 438–448

Contents lists available at ScienceDirect

Applied Mathematical Modelling

journal homepage: www.elsevier.com/locate/apm

Development of approximate solutions for contaminant transport through fractured media

Chih-Tien Liu [1], Hund-Der Yeh *

Institute of Environmental Engineering, National Chiao Tung University, Hsinchu 300, Taiwan

ARTICLE INFO

Article history:
Received 1 May 2013
Received in revised form 5 February 2014
Accepted 27 May 2014
Available online 12 June 2014

Keywords:
Approximate solution
Padé approximation
Laplace transform
Small-time
Large-time

ABSTRACT

Approximate solutions are sometimes very convenient and useful in engineering practices if the analytical solution is in a complicated form and difficult to evaluate accurately. This study develops four different approximate solutions for the problem of contaminant transport in fractured media presented in Tang et al. (1981) [1]. Their problem was solved analytically and the solutions of concentration distributions in the fracture and the rock expressed in infinite integrals had to rely on numerical approaches to obtain the results. The approximate solutions we develop herein include small-time solution, large-time solution, low-order approximate solution and high-order one based on the Padé approximation technique. The small-time solution gives very accurate concentrations at early times while the large-time solution yields excellent predictions at late times, as compared to Tang et al.'s solution (Tang et al., 1981) [1]. In contrast, the solution based on low-order Padé approximation with polynomials of degree one in the numerator and degree two in the denominator gives fairly good predictions over the entire time domain, especially in the intermediate period as compared with those of the small-time and large-time solutions. In addition, the solution based on high-order Padé approximation with polynomials of degree two in the numerator and degree three in the denominator is also developed and its predicted concentrations are also compared with Tang et al.'s solution (Tang et al., 1981) [1]. These results reveal that the Padé approximation has an advantage of being capable of producing more accurate results than the relationships of *SPLT* and *LPST* in the intermediate and late time periods.

1. Introduction

Fracture–matrix interactions can significantly affect contaminant transport in fractured porous media and rock matrix. In the past several decades, many attempts had been made at developing analytical models based on the advection–dispersion equation for investigating the contaminants migration and fate in fractured media. The solutions of the model commonly solved by the Laplace transform technique were used to predict the concentration distributions of the contaminants in the fracture–matrix systems. Due to complexity, some Laplace-domain solutions are difficult to invert to real time domain analytically. Moreover, a few time-domain solutions expressed in terms of infinite integrals or double integrals with complicated integrands are rather arduous to evaluate accurately (e.g., [1–5]). The first analytical treatment in a fractured media

* Corresponding author. Tel.: +886 3 5731910; fax: +886 3 5725958/6050.
E-mail address: hdyeh@mail.nctu.edu.tw (H.-D. Yeh).
[1] Tel.: +886 3 5731910; fax: +886 3 5726050.

http://dx.doi.org/10.1016/j.apm.2014.05.041
0307-904X/

may be attributed to Tang et al. [1], who presented analytical solutions in a single fracture imbedded in infinite matrix by taking into account advection, dispersion, molecular diffusion, adsorption and radioactive decay. The effect of longitudinal dispersion on contaminant penetration distances along fracture and into rock matrix was discussed and compared. Their solution was extended by Sudicky and Frind [2] to account for the presence of adjacent parallel fractures. Their solutions for the fracture and rock matrix were, however, expressed in terms of an infinite integral or a double integral with a complicated integrand which relies on numerical integration to obtain the results. Note that Davis and Johnston [4] gave a comment on the errors in the analytical expressions developed by Sudicky and Frind [2] and presented the correct solutions for the concentration in the porous matrix.

To develop the approximate solutions, Yeh and Chang [6] mentioned three different approaches including the approximations to the governing equation, to the Laplace domain solution, and to the time domain solution. The use of perturbation method for deriving the approximate solution allows hard problems in terms of the mathematical model to be solved by perturbing easier problems as demonstrated by Farlow [7]. Batu and Van Genuchten [8] adopted a singular perturbation method to solve the Boussinesq equation for a constant injection into a radial aquifer. Moutsopoulos and Tsihrintzis [9] derived approximate solutions for transient flow through porous media by applying the perturbation technique. The approximate solution derived from the perturbation approach is generally applicable over the entire time domain. In the areas of groundwater and heat flow, the relationship of large p (Laplace variable) vs. small t (hereinafter referred to as *LPST*) is commonly applied to the Laplace-domain solution to determine the small-time solution while the relationship of small p vs. large t (hereinafter referred to as *SPLT*) is employed to develop the large-time solution. Wallach and Parlange [10] applied the *LPST* relationship to obtain the small-time solutions for the problem of contaminant transport in a crack/matrix system. Yeh and Wang [11] presented a short review on the applications of *LPST*, *SPLT*, and both to groundwater flow problems for obtaining the approximate solutions. The methods of series expansion (e.g., [12]) and asymptotic expansion (e.g., [13]) are also commonly used to find the approximate time-domain solutions. Akin and Counts [14] and Longman [15] presented a procedure to obtain rational approximations of the inverse Laplace transform by utilizing Taylor series expansion. Heavilin and Neilson [16] used a rational expression to approximate the Laplace-domain solution for the problem of heat transport in a stream system. Their solution method can be considered as a simplified approach of Padé approximation.

The objective of this study is to develop four different approximate solutions for ease of computation. They are a small-time solution, a large-time solution, a low-order Padé approximation solution and a high-order one. The small-time solution and large-time solution are derived based on the relationships of *LPST* and *SPLT*, respectively. Comparisons of temporal distributions of the dimensionless concentration predicted from the approximate solutions and Tang et al.'s solution [1] indicate that approximate solutions have good results over some specific time ranges. These approximate solutions have simpler forms than the analytical solutions and are much easier in evaluating the transient behavior of contaminant transport with desired accuracy.

2. Problem of contaminant migrating in a fractured medium

2.1. Laplace domain solution of contaminant concentration

Tang et al. [1] considered tritium (^3H) transport from an injection well into a thin rigid fracture situated in a saturated porous rock as shown in Fig. 1. The transport processes considered in their mathematical model included the advection in the fracture, longitudinal dispersion in the fracture, molecular diffusion from the fracture into the rock matrix, adsorption and radioactive decay. Certain assumptions were made to allow the model formulated as two coupled, one-dimensional partial differential equations: one was for the fracture while the other for the rock matrix, which extends both along and perpendicular to the fracture.

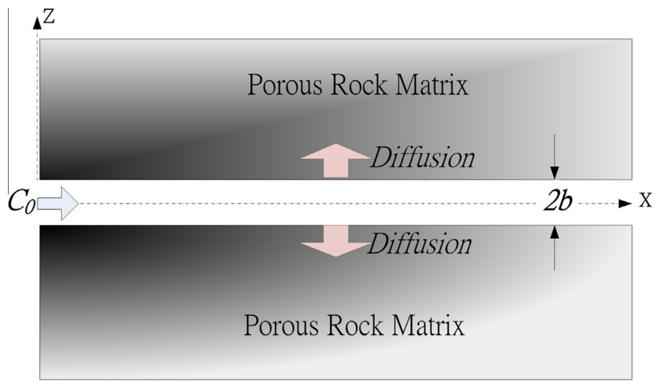

Fig. 1. Schematic representation of the fracture and porous rock matrix.

The governing equation for the Laplace transformation of solute concentration ($\bar{C}_f$) in the fracture is expressed as

$$\frac{d^2\bar{C}_f}{dx^2} - \frac{v}{D}\frac{d\bar{C}_f}{dx} - \left(\frac{R}{D}(p+\lambda) + \frac{\theta\sqrt{R_r D_r}}{bD}\sqrt{p+\lambda}\right)\bar{C}_f = 0, \tag{1}$$

$$\bar{C}_f(0,p) = \frac{C_0}{p}, \tag{2}$$

$$\bar{C}_f(\infty,p) = 0, \tag{3}$$

where p is the Laplace variable; v is the groundwater velocity in the fracture; λ is the radioactive decay constant; θ is the porosity of the rock matrix; D the hydrodynamic dispersion coefficient defined as $D = \alpha_L v + D^*$ with α_L the longitudinal dispersivity and D^* the molecular diffusion coefficient; D_r is the effective micro-pore diffusion coefficient defined as $D_r = \tau D^*$ with the matrix tortuosity τ; R and R_r are the retardation factors in the fracture and rock matrix, respectively; C_0 is the source concentration.

The governing equation for the Laplace transformation of solute concentration ($\bar{C}_r$) in the rock matrix is

$$\frac{d^2\bar{C}_r}{dz^2} - \frac{R_r}{D_r}(p+\lambda)\bar{C}_r = 0, \tag{4}$$

$$\bar{C}_r(b,p) = \bar{C}_f(x,p), \tag{5}$$

$$\bar{C}_r(\infty,p) = 0. \tag{6}$$

The Laplace domain solutions for the fracture and the rock matrix are expressed, respectively, as [1]

$$\bar{C}_f(x,p) = \frac{C_0}{p}\exp\left(\nu x - x\sqrt{\nu^2 + \kappa(p+\lambda) + \varepsilon(p+\lambda)^{1/2}}\right), \tag{7}$$

and

$$\bar{C}_r(z,p) = \bar{C}_f(x,p)\exp\left(-(z-b)\sqrt{\kappa_r(p+\lambda)}\right), \tag{8}$$

where $\nu = v/2D$, $\kappa = R/D$, $\kappa_r = R_r/D_r$, and $\varepsilon = \theta\sqrt{R_r D_r}/bD$.

The time domain solution for the fracture is [1]

$$\frac{C_f}{C_0} = \frac{\exp(\nu x)}{\sqrt{\pi}}\int_l^\infty \exp\left(-\xi^2 - \frac{\nu^2 x^2}{4\xi^2} - \eta x^2\right)\left\{\begin{array}{l}\exp(-\lambda^{1/2}Y)erfc\left(\frac{Y}{2T} - \lambda^{1/2}T\right) \\ +\exp(\lambda^{1/2}Y)erfc\left(\frac{Y}{2T} + \lambda^{1/2}T\right)\end{array}\right\}d\xi, \tag{9}$$

where $l = x\sqrt{\kappa/t}/2$, $\eta = \lambda\kappa/4\xi^2$, $Y = \nu^2\beta^2x^2A/4\xi^2$, $A = \theta\sqrt{R_r D_r}/bR$, $\beta^2 = 4RD/v^2$, and $T = \sqrt{t - \kappa x^2/4\xi^2}$. The solution for the rock-matrix can be written as [1]

$$\frac{C_r}{C_0} = \frac{\exp(\nu x)}{\sqrt{\pi}}\int_l^\infty \exp\left(-\xi^2 - \frac{\nu^2 x^2}{4\xi^2} - \eta x^2\right)\left\{\begin{array}{l}\exp(-\lambda^{1/2}Y')erfc\left(\frac{Y'}{2T} - \lambda^{1/2}T\right) \\ +\exp(\lambda^{1/2}Y')erfc\left(\frac{Y'}{2T} + \lambda^{1/2}T\right)\end{array}\right\}d\xi, \tag{10}$$

where $Y' = Y + \sqrt{\kappa_r}(z-b)$. These two solutions are in terms of infinite integrals with complicated integrands and have to rely on numerical evaluations.

2.2. Small-time solution of contaminant concentration

In this section the perturbation method and the relationship of *LPST* are applied to Eq. (1) with considering the perturbation parameter denoted as ω which equals $\theta\sqrt{R_r D_r}/D$. Assume the solution of Eq. (1) can be expanded as following perturbation series

$$\bar{C}_f(x,p) = \bar{f}_0(x,p) + \omega\bar{f}_1(x,p) + \omega^2\bar{f}_2(x,p) + \cdots \tag{11}$$

Substitute Eq. (11) into Eqs. (1)–(3) and expand the left-hand side (LHS) of the resulting equations in power series of ε as, respectively,

$$\frac{d^2}{dx^2}(\bar{f}_0 + \omega\bar{f}_1 + \cdots) - 2\nu\frac{d}{dx}(\bar{f}_0 + \omega\bar{f}_1 + \cdots) - \left(\kappa(p+\lambda) + \omega\frac{\sqrt{p+\lambda}}{b}\right)(\bar{f}_0 + \omega\bar{f}_1 + \cdots) = 0, \tag{12}$$

$$\bar{f}_0(0,p) + \omega\bar{f}_1(0,p) + \cdots = 1/p, \tag{13}$$

$$\bar{f}_0(\infty, p) + \omega \bar{f}_1(\infty, p) + \cdots = 0. \tag{14}$$

According to the assumption of perturbation technique that the perturbation parameter is small and the perturbation series is rapidly convergent, therefore, the high-order terms in the series are negligible when ω is small. The first and the second terms in the perturbation series lead to the zero-order and first-order perturbations, respectively, when equating terms multiplied by ω^0 and ω^1 in Eqs. (12)–(14) as

$$\frac{d^2\bar{f}_0}{dx^2} - 2v\frac{d\bar{f}_0}{dx} - \kappa(p+\lambda)\bar{f}_0 = 0, \tag{15}$$

$$\bar{f}_0(0, p) = 1/p, \tag{16}$$

$$\bar{f}_0(\infty, p) = 0, \tag{17}$$

and

$$\frac{d^2\bar{f}_1}{dx^2} - 2v\frac{d\bar{f}_1}{dx} - \kappa(p+\lambda)\bar{f}_1 = \frac{\sqrt{p+\lambda}}{b}\bar{f}_0, \tag{18}$$

$$\bar{f}_1(0, p) = 0, \tag{19}$$

$$\bar{f}_1(\infty, p) = 0. \tag{20}$$

The Laplace-domain solutions for the unknowns $\bar{f}_0(x,p)$ and $\bar{f}_1(x,p)$ can be obtained by solving the homogeneous and non-homogeneous linear second-order ODEs. The zero-order perturbation can be obtained as

$$\bar{f}_0(x, p) = \frac{1}{p}\exp(x(v - \sqrt{\kappa(p+\alpha)})). \tag{21}$$

Substituting the zero-order perturbation, Eq. (21), into the RHS in Eq. (18), the non-homogeneous linear second-order ODEs can be solved by homogeneous solution and particular solution separately. The first-order perturbation can then be expressed as

$$\bar{f}_1(x, p) = \frac{-x}{2b\sqrt{\kappa}}\sqrt{\frac{p+\lambda}{p+\alpha}}\frac{1}{p}\exp(x(v - \sqrt{\kappa(p+\alpha)})), \tag{22}$$

where $\alpha = v^2/(4DR) + \lambda$.

Substituting Eqs. (21) and (22) into Eq. (11), the Laplace-domain solution in the fracture can be expressed as

$$\frac{\bar{C}_f(x,p)}{C_0} = \left(1 - \frac{\omega x}{2b\sqrt{\kappa}}\sqrt{\frac{p+\lambda}{p+\alpha}}\right)\frac{1}{p}\exp(x(v - \sqrt{\kappa(p+\alpha)})). \tag{23}$$

The Taylor series expansion for $\sqrt{(p+\lambda)/(p+\alpha)}$ in Eq. (23) results in $\sqrt{(p+\lambda)/(p+\alpha)} = 1 + (\lambda-\alpha)/2(p+\alpha) - (\lambda-\alpha)^2/8(p+\alpha)^2 + \cdots$ and then substituting the series into Eq. (23) yields

$$\frac{\bar{C}_f(x,p)}{C_0} = \left(\frac{1}{p} - \frac{\omega x}{2b\sqrt{\kappa}}\left(\frac{1}{p} + \sigma\left(\frac{1}{p} - \frac{1}{p+\alpha}\right) - \frac{\sigma^2}{2}\left(\frac{1}{p} - \frac{1}{p+\alpha} - \frac{\alpha}{(p+\alpha)^2}\right)\right)\right)\exp(x(v - \sqrt{\kappa(p+\alpha)})), \tag{24}$$

where $\sigma = (\lambda - \alpha)/2\alpha$.

Note that the higher-order terms of p may be negligible when p is large. Consequently, Eq. (24) can be written as

$$\frac{\bar{C}_f(x,P)}{C_0} = \left(\frac{\eta_1}{P} + \frac{\eta_2}{P-\alpha}\right)\exp(x(v - \sqrt{\kappa}P^{1/2})), \tag{25}$$

where $P = p + \alpha$, $\eta_1 = \omega x(\sigma - \sigma^2/2)/2b\sqrt{\kappa}$, and $\eta_2 = 1 - \eta_1 - (\omega x/2b\sqrt{\kappa})$.

The small-time solution for contaminant concentration in the fracture can then be obtained after taking the inverse Laplace transform to Eq. (25) with two inverse Laplace transform formulas given in Carslaw and Jaeger [17]

$$\frac{C_f(x,t)}{C_0} = \eta_1 \exp\left(\frac{vx}{2D}\right) erfc\left(\frac{Rx}{\sqrt{4DRt}}\right) + \frac{\eta_2}{2}\exp(\alpha t)\left\{\begin{array}{l} \exp\left(\frac{(v-\varpi_1)x}{2D}\right) erfc\left(\frac{Rx-\varpi_1 t}{\sqrt{4DRt}}\right) \\ + \exp\left(\frac{(v+\varpi_1)x}{2D}\right) erfc\left(\frac{Rx+\varpi_1 t}{\sqrt{4DRt}}\right) \end{array}\right\}, \tag{26}$$

where $\varpi_1 = \sqrt{v^2 + 4DR\lambda}$

Substituting Eq. (25) into Eq. (8) yields the Laplace-domain solution for the rock matrix as

$$\frac{\bar{C}_r}{C_0}=\left(\frac{\eta_1}{P}+\frac{\eta_2}{P-\alpha}\right)\exp(x(\upsilon-\sqrt{\kappa}P^{1/2}))\exp\left(-(z-b)\sqrt{\kappa_r}\left(P-\frac{\upsilon^2}{4DR}\right)^{1/2}\right). \tag{27}$$

Taking the Taylor series expansion for $(P-\upsilon^2/4DR)^{1/2}$ in Eq. (27) and neglecting the second and higher-order terms for large values of P results in $(P-\upsilon^2/4DR)^{1/2}\approx P^{1/2}$. Eq. (27) can then be reduced to

$$\frac{\bar{C}_r}{C_0}=\left(\frac{\eta_1}{P}+\frac{\eta_2}{P-\alpha}\right)\exp(\upsilon x-\zeta P^{1/2}), \tag{28}$$

where $\zeta=x\sqrt{\kappa}+(z-b)\sqrt{\kappa_r}$.

The small-time solution for the rock matrix can be obtained after taking the inverse Laplace transform to Eq. (28) as

$$\frac{C_r(z,t)}{C_0}=\eta_1\exp\left(\frac{\upsilon x}{2D}\right)erfc\left(\frac{\zeta}{2\sqrt{t}}\right)+\frac{\eta_2}{2}\exp(\alpha t)\left\{\begin{array}{l}\exp\left(\frac{\upsilon x}{2D}-\zeta\sqrt{\alpha}\right)erfc\left(\frac{\zeta}{2\sqrt{t}}-\sqrt{\alpha t}\right)\\+\exp\left(\frac{\upsilon x}{2D}+\zeta\sqrt{\alpha}\right)erfc\left(\frac{\zeta}{2\sqrt{t}}+\sqrt{\alpha t}\right)\end{array}\right\}. \tag{29}$$

The small-time solutions of Eqs. (26) and (29) consisted of exponential function and complementary error function have simpler forms than the solutions expressed in terms of an infinite integral developed by Tang et al. [1] shown in Eqs. (9) and (10).

2.3. Large-time solution of contaminant concentration

Similarly, the large-time solution can be developed based on the Laplace-domain solution using series expansion and the *SPLT* relationship. The Taylor series expansion for $(p+\lambda)^{1/2}$ inside the square root of Eq. (7) yields $(p+\lambda)^{1/2}=\lambda^{1/2}(1+p/2\lambda-p^2/8\lambda^2+\cdots)$ subject to the constraint of $p<\lambda$ for $(1+p/\lambda)^{1/2}$. Likewise, the third and higher-order terms may be neglected when p is small. Eq. (7) can be reduced to

$$\frac{\bar{C}_f(x,p)}{C_0}=\exp(\upsilon x)\frac{\exp\left(-x\sqrt{\kappa}\sqrt{\alpha+A\lambda^{1/2}+\beta p}\right)}{p}, \tag{30}$$

where $\beta=1+A/2\lambda^{1/2}$.

The solution for dimensionless concentration in the fracture can then be obtained by inverting the solution in Eq. (30) using the formula given in Oberhettinger and Badii [18]. The result is

$$\frac{C_f(x,t)}{C_0}=\frac{1}{2}\left\{\exp\left(\frac{(\upsilon-\varpi_2)x}{2D}\right)erfc\left(\frac{\beta Rx-\varpi_2 t}{\sqrt{4DR\beta t}}\right)+\exp\left(\frac{(\upsilon+\varpi_2)x}{2D}\right)erfc\left(\frac{\beta Rx+\varpi_2 t}{\sqrt{4DR\beta t}}\right)\right\}, \tag{31}$$

where the lumped parameter $\varpi_2=\sqrt{\upsilon^2+4DR(\lambda+A)}$.

Substituting Eq. (30) into Eq. (8) and neglecting the third and higher-order terms of Taylor series expansion for $(p+\lambda)^{1/2}$ inside the square root of Eq. (8) yields the Laplace-domain solution for the rock matrix at late times

$$\frac{\bar{C}_r(z,p)}{C_0}=\exp\left(\upsilon x-(z-b)\sqrt{\kappa_r\lambda}\right)\frac{1}{p}\exp\left(-x\sqrt{\kappa}\sqrt{\alpha+A\lambda^{1/2}+\beta p}-\frac{1}{2}\sqrt{\frac{\kappa_r}{\lambda}}p\right). \tag{32}$$

The large-time solution for contaminant concentration in the rock matrix is subsequently obtained after taking the inverse Laplace transform to Eq. (32) as

$$\frac{C_r(z,t)}{C_0}=\frac{\exp\left(-\sqrt{\kappa_r\lambda}(z-b)\right)}{2}\left\{\begin{array}{l}\exp\left(\frac{(\upsilon-\varpi_1)x}{2D}\right)erfc\left(\frac{\beta Rx-\varpi_1 t}{\sqrt{4DR\beta t}}\right)\\+\exp\left(\frac{(\upsilon+\varpi_1)x}{2D}\right)erfc\left(\frac{\beta Rx+\varpi_1 t}{\sqrt{4DR\beta t}}\right)\end{array}\right\}\delta(T), \tag{33}$$

where $\delta(T)$ is a delayed unit step function and $T=t-\sqrt{\kappa_r\lambda}(z-b)/2\lambda$.

The large-time solutions for both the fracture and rock matrix are simpler than Tang et al.'s solutions [1] and much easier to evaluate the transient behavior of contaminant transport at late times.

2.4. Padé approximation solution

Consider that a function of $F(x)$ defined over an interval $a\leqslant x\leqslant b$ is approximated by a rational function in the form of $F(x)=P(x)/Q(x)$, where $P(x)$ and $Q(x)$ are polynomials with no common zeros.

$$F(x)=\frac{P_m(x)}{Q_n(x)}=\frac{a_0+a_1x+a_2x^2+\cdots+a_mx^m}{1+b_1x+b_2x^2+\cdots+b_nx^n}. \tag{34}$$

The constant term in the denominator b_0 can be taken as unity without loss of generality [19], because it can always obtain this form by dividing both numerator and denominator by b_0. Herein we begin by expanding the argument, p, in the exponential function on Eq. (7), $\bar{f}(x,p) = \exp\left[x\left(v - \sqrt{v^2 + \kappa(p+\lambda) + \varepsilon(p+\lambda)^{1/2}}\right)\right]$, and equate this expansion to a rational function with a polynomial of degree two in the denominator and a polynomial of degree one in the numerator.

The Maclaurin series expansion for the argument, p, within the exponential function in $\bar{f}(x,p)$ can be expressed as

$$\bar{f}(x,p) = \exp[x(v-\gamma)](1 - pg_1(x) + p^2 g_2(x) - p^3 g_3(x) + \cdots), \tag{35}$$

with

$$g_1(x) = \frac{\rho x}{2\gamma}, \tag{36}$$

$$g_2(x) = \frac{1}{2!}\left((\gamma^{-3}x + \gamma^{-2}x^2)\frac{\rho^2}{4} + \frac{\gamma^{-1}\varepsilon x}{8\lambda^{3/2}}\right), \tag{37}$$

$$g_3(x) = \frac{1}{3!}\left((3\gamma^{-5}x + 3\gamma^{-4}x^2 + \gamma^{-3}x^3)\frac{\rho^3}{8} + (3\gamma^{-3}x + 3\gamma^{-2}x^2)\frac{\varepsilon\rho}{16\lambda^{3/2}} + \frac{3\gamma^{-1}\varepsilon x}{16\lambda^{5/2}}\right), \tag{38}$$

where $\gamma = \sqrt{v^2 + \kappa\lambda + \varepsilon\lambda^{1/2}}$ and $\rho = \kappa + (\varepsilon/2\lambda^{1/2})$.

Equating the Maclaurin series expansion to the low-order rational function described above results in

$$\bar{f}(x,p) = \exp[x(v-\gamma)](1 - pg_1(x) + p^2 g_2(x) - p^3 g_3(x)) \approx \exp[x(v-\gamma)]\frac{1 + a_1 p}{1 + b_1 p + b_2 p^2}. \tag{39}$$

Multiplying both sides by $1 + b_1 p + b_2 p^2$ and arranging the powers of p yields the coefficients appearing on the RHS of Eq. (39) as

$$a_1 = \frac{2g_1 g_2 - g_3 - g_1^3}{g_1^2 - g_2}, \tag{40}$$

$$b_1 = \frac{g_1 g_2 - g_3}{g_1^2 - g_2}, \tag{41}$$

$$b_2 = \frac{g_2^2 - g_1 g_3}{g_1^2 - g_2}. \tag{42}$$

With Eqs. (39)–(42), $\bar{C}_f(x,p)$ in Eq. (7) can be approximated as

$$\frac{\bar{C}_f(x,p)}{C_0} = \exp(x(v-\gamma))\left[\frac{1}{p} + \frac{A}{p+\varsigma_1} - \frac{A+1}{p+\varsigma_2}\right], \tag{43}$$

with

$$A = \frac{a_1/b_2 - \varsigma_2}{2\varsigma_2 - (b_1/b_2)}, \tag{44}$$

$$\varsigma_1 = \frac{b_1}{2b_2} - \sqrt{\left(\frac{b_1}{2b_2}\right)^2 - \frac{1}{b_2}}, \tag{45}$$

$$\varsigma_2 = \frac{b_1}{2b_2} + \sqrt{\left(\frac{b_1}{2b_2}\right)^2 - \frac{1}{b_2}}. \tag{46}$$

Finally, the low-order Padé approximation solution for the fracture after taking the inverse Laplace transform to Eq. (43) can be obtained as

$$\frac{C_f(x,t)}{C_0} = \exp(x(v-\gamma))[1 + A\exp(-\varsigma_1 t) - (A+1)\exp(-\varsigma_2 t)]. \tag{47}$$

Similarly, the exponential function on the RHS of Eq. (8), $\bar{f}_r(z,p) = \exp\left[x\left(v - \sqrt{v^2 + \kappa(p+\lambda) + \varepsilon(p+\lambda)^{1/2}}\right) - (z-b)\sqrt{\kappa_r(p+\lambda)}\right]$, is developed as the Maclaurin series and equates this series to a low-order rational function

$$\begin{aligned} \bar{f}_r(z,p) &= \exp\left[x(v-\gamma) - (z-b)\sqrt{\kappa_r\lambda}\right](1 - ph_1(x) + p^2 h_2(x) - p^3 h_3(x)) \\ &\approx \exp\left[x(v-\gamma) - (z-b)\sqrt{\kappa_r\lambda}\right]\frac{1 + c_1 p}{1 + d_1 p + d_2 p^2} \end{aligned}, \tag{48}$$

with

$$h_1(x) = \frac{\rho x}{2\gamma} + (z-b)\frac{\kappa_r^{1/2}}{2\lambda^{1/2}}, \tag{49}$$

$$h_2(x) = \frac{1}{2!}\left(\frac{\gamma^{-3}x\rho^2}{4} + \frac{\gamma^{-1}\varepsilon x}{8\lambda^{3/2}} + (z-b)\frac{\kappa_r^{1/2}}{4\lambda^{3/2}} + h_1^2(x)\right), \tag{50}$$

$$h_3(x) = \frac{1}{3!}\left(\begin{array}{l} \frac{3\gamma^{-5}x\rho^3}{8} + \frac{3\gamma^{-3}\varepsilon x\rho}{16\lambda^{3/2}} + \frac{3\gamma^{-1}\varepsilon x}{16\lambda^{5/2}} + (z-b)\frac{3\kappa_r^{1/2}}{8\lambda^{5/2}} \\ + \left[\frac{\gamma^{-3}x\rho^2}{4} + \frac{\gamma^{-1}\varepsilon x}{8\lambda^{3/2}} + (z-b)\frac{\kappa_r^{1/2}}{4\lambda^{3/2}}\right]h_1(x) + h_1^3(x) \end{array}\right), \tag{51}$$

and

$$c_1 = \frac{2h_1h_2 - h_3 - h_1^3}{h_1^2 - h_2}, \tag{52}$$

$$d_1 = \frac{h_1h_2 - h_3}{h_1^2 - h_2}, \tag{53}$$

$$d_2 = \frac{h_2^2 - h_1h_3}{h_1^2 - h_2}. \tag{54}$$

Accordingly, the Laplace-domain solution for the rock matrix can be obtained as

$$\frac{\bar{C}_r(z,p)}{C_0} \approx \exp\left[x(v-\gamma) - (z-b)\sqrt{\kappa_r\lambda}\right]\cdot\left[\frac{1}{p} + \frac{B}{p+\varsigma_3} - \frac{B+1}{p+\varsigma_4}\right], \tag{55}$$

with

$$B = \frac{c_1/d_2 - \varsigma_4}{2\varsigma_4 - (d_1/d_2)}, \tag{56}$$

$$\varsigma_3 = \frac{d_1}{2d_2} - \sqrt{\left(\frac{d_1}{2d_2}\right)^2 - \frac{1}{d_2}}, \tag{57}$$

$$\varsigma_4 = \frac{d_1}{2d_2} + \sqrt{\left(\frac{d_1}{2d_2}\right)^2 - \frac{1}{d_2}}. \tag{58}$$

The low-order Padé approximation solution for the rock matrix after taking the inverse Laplace transform can then be obtained as

$$\frac{C_r(z,t)}{C_0} = \exp\left[x(v-\gamma) - (z-b)\sqrt{\kappa_r\lambda}\right][1 + B\exp(-\varsigma_3 t) - (B+1)\exp(-\varsigma_4 t)]. \tag{59}$$

Note that both approximate solutions for concentration distributions in the fracture and the rock matrix are closed-form and much easier to evaluate when compared with the solutions given by Tang et al. [1].

The expression for the truncation error made by Padé approximation solution to a function is given [20]

$$R_{m,n}(t) = \frac{P_m(t)}{Q_n(t)} - F(t). \tag{60}$$

To estimate the truncation errors incurred in the Padé approximation solution, a high-order Padé approximation solution with polynomials of degree two in the nominator and degree three in the denominator is also adopted as follow

$$\frac{\bar{C}_f(x,p)}{C_0} = \exp(x(v-\gamma))\frac{1 + \hat{a}_1p + +\hat{a}_2p^2}{1 + \hat{b}_1p + \hat{b}_2p^2 + \hat{b}_3p^3}, \tag{61}$$

with

$$\hat{a}_1 = \hat{b}_1 - g_1, \tag{62}$$

$$\hat{a}_2 = \hat{b}_2 - g_1\hat{b}_1 + g_2, \tag{63}$$

$$\hat{b}_1 = \frac{(g_1g_3 - g_4)(g_1g_2 - g_3) + (g_2g_3 - g_5)(g_2 - g_1^2)}{(g_1g_2 - g_3)^2 - (g_4 - g_2^2)(g_2 - g_1^2)}, \tag{64}$$

$$\hat{b}_2 = \frac{(g_1g_3 - g_4) - \hat{b}_1(g_1g_2 - g_3)}{(g_2 - g_1^2)}, \tag{65}$$

$$\hat{b}_3 = g_1\hat{b}_2 - g_2\hat{b}_1 + g_3, \tag{66}$$

where $g_4(x) = \frac{1}{4!}\begin{pmatrix} (15\gamma^{-7}x + 15\gamma^{-6}x^2 + 6\gamma^{-5}x^3 + \gamma^{-4}x^4)\frac{\rho^4}{16} + (9\gamma^{-5}x + 9\gamma^{-4}x^2 + 3\gamma^{-3}x^3)\frac{\varepsilon\rho^2}{16\lambda^{3/2}} \\ +(\gamma^{-3}x + \gamma^{-2}x^2)\frac{3\varepsilon\rho}{8\lambda^{5/2}} + (\gamma^{-3}x + \gamma^{-2}x^2)\frac{3\varepsilon^2}{64\lambda^3} + \frac{15\gamma^{-1}x\varepsilon}{32\lambda^{7/2}} \end{pmatrix}$, and

$$g_5(x) = \frac{1}{5!}\begin{pmatrix} (105\gamma^{-9}x + 105\gamma^{-8}x^2 + 45\gamma^{-7}x^3 + 10\gamma^{-6}x^4 + \gamma^{-5}x^5)\frac{\rho^5}{32} \\ +(15\gamma^{-7}x + 15\gamma^{-6}x^2 + 6\gamma^{-5}x^3 + \gamma^{-4}x^4)\frac{5\varepsilon\rho^3}{32\lambda^{3/2}} + (3\gamma^{-5}x + 3\gamma^{-4}x^2 + \gamma^{-3}x^3)\frac{15\varepsilon\rho^2}{32\lambda^{5/2}} \\ +(3\gamma^{-5}x + 3\gamma^{-4}x^2 + \gamma^{-3}x^3)\frac{15\varepsilon^2\rho}{128\lambda^3} + (\gamma^{-3}x + \gamma^{-2}x^2)\frac{75\varepsilon\rho}{64\lambda^{7/2}} + (\gamma^{-3}x + \gamma^{-2}x^2)\frac{15\varepsilon^2}{64\lambda^4} + \frac{105\gamma^{-1}x\varepsilon}{64\lambda^{9/2}} \end{pmatrix}.$$

The inversion routine DINLAP of IMSL [21] was developed based on a numerical algorithm originally proposed by Crump [22] and later modified by de Hoog et al. [23]. The DINLAP is used to evaluate the time-domain results of Eqs. (7), (43), and (61) with accuracy to the sixth decimal. This algorithm approximates Laplace inversion of the inverted function in a Fourier series and accelerates the computation using Shanks method [24]. Note that the routine DINLAP has been successfully applied in groundwater area (e.g., [5]).

3. Results and discussion

A hypothetical case concerning tritium (^3H) transport in fractured medium due to well injection is chosen to illustrate the applications of the developed approximate solutions. The hydrogeological parameters used in the case are listed in Table 1. The results predicted by the small-time, large-time solutions, low-order Padé approximation solution and high-order one are compared with Tang et al.'s solution (Eqs. (9) and (10)) evaluated by Gaussian quadrature with 60 Gauss points.

Fig. 2a shows the temporal distributions of contaminant concentration in the fracture predicted by Tang et al.'s solution and the respective approximate solutions given in Eqs. (26), (31), (47), and (61) at the location of $x = 1$ m. The figure shows that the small-time solution (Eq. (26)) matches with the analytical solution prior to $t = 2$ years and the large-time solution (Eq. (31)) shows excellent agreement with the Tang et al.'s solution after about $t = 7$ years. In addition, the Padé approximation solutions (Eqs. (47) and (61)) give fairly good results when compared with those predicted by the small-time and large-time solutions as indicated in the figure. However, the predicted concentration of small-time solution gets more accuracy than the Padé approximation solutions prior $t = 0.1$ year. Steady state is essentially attained after about $t = 20$ years for this specific condition. To examine the accuracy, absolute errors of the predicted concentrations are subsequently calculated as shown in Fig. 2b. As expected, the predicted error of the small-time solution increases with elapsed time, from 2.3% at $t = 2$ years to 7% at $t = 14$ years. In addition, the error made by the large-time solution is large at early times, but gradually decreases as time increases, and finally becomes negligible after 7 years. Over the entire time period, the errors made by the low-order Padé approximation or high-order one are always less than 3% after $t = 2$ years.

Fig. 3 demonstrates the comparisons of predicted concentrations from four different solutions within the rock matrix at the location $x = 1$ m and $z = 0.1$ m. This figure shows close agreement between the Padé approximation solution (Eq. (59)) and Tang et al.'s solution (Eq. (10)) for estimated tritium concentrations over the entire elapsed times. The absolute error in predicted concentration in the rock matrix is less than 3% before $t = 6$ years for the small-time solutions and after

Table 1
Parameter values for the fracture and rock matrix.

Parameters	Values
Fracture half-aperture, b	5×10^{-4} m
Average velocity of groundwater in the fracture, v	0.01 m/day
Half-life of ^3H, $T_{1/2}$	12.35 years
Longitudinal dispersivity in the fracture axis, α_L	0.5 m
Coefficient of molecular diffusion in water, D^*	5.475×10^{-5} m^2/day
Tortuosity of rock matrix, τ	0.1
Retardation factor, R	1.0
Rock-matrix retardation factor, R_r	1.0
Porosity of rock matrix, θ	0.01

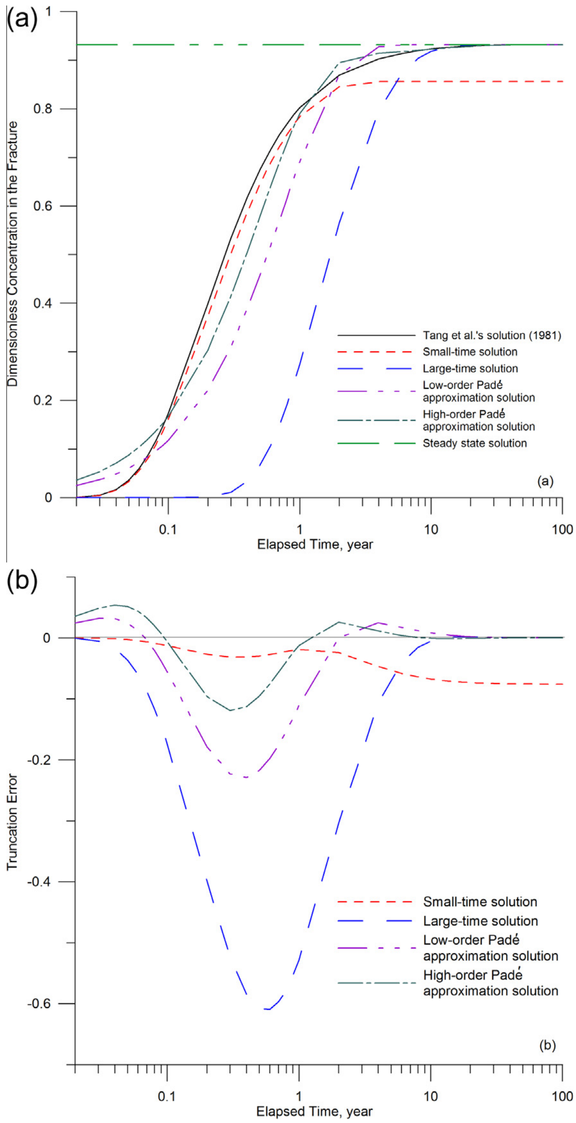

Fig. 2. (a) Predicted temporal concentration distributions in the fracture by the approximate solutions and Tang et al.'s solution [1]. (b) Truncation errors estimated by the respective approximate solutions given in Eqs. (26), (31), (47), and (61) as compared to the Tang et al.'s solution [1].

$t = 16$ years for the large-time solutions. The error made by the Padé approximation solution is greater than 5% prior to $t = 1$ year, but it gradually decreases as time increases and finally matches with the results predicted by Tang et al. [1]. Those results demonstrated that the proposed approximate solutions provide a simple and useful tool for simulating contaminant transport through the fractured media.

In Fig. 4, we compare the contaminant concentrations in the fracture predicted by the low-order Padé approximation solution (Eq. (47)) and the high-order one (Eq. (61)) and Tang et al.'s solution (Eq. (9)). The results reveal that prior to $t = 0.1$ year, the predicted concentration by the low-order Padé approximation solution is slightly better than the high-order one. The truncation errors made by the low-order Padé approximation and high-order one are −6.979E−03 and −1.994E−02 at $t = 0.09$ year, respectively. In the intermediate period, on the contrary, the predicted concentration by the high-order Padé approximation solution is mildly better than the low-order one. The errors made by Eq. (61) are smaller than those of Eq. (47) at $t = 0.9$ year, which are 8.089E−03 and 2.438E−02, respectively. In addition, the low-order and high-order Padé approximation solutions give excellent results in late times as compared with Tang et al.'s solution. The results show that the low-order Padé approximation solution is acceptable with smaller errors when compared the high-order one.

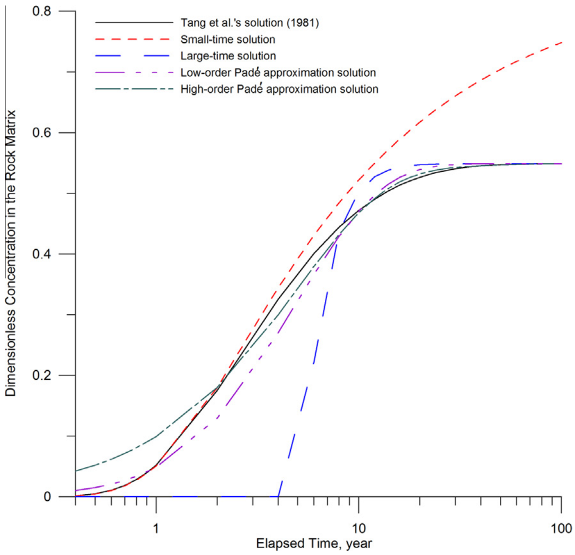

Fig. 3. Predicted temporal concentration distributions within the rock matrix by the approximate solutions and Tang et al.'s solution [1] at $(x, z) = (1, 0.1 \text{ m})$.

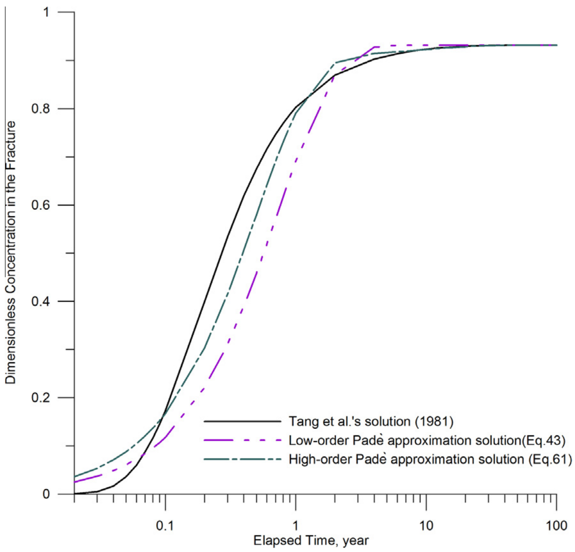

Fig. 4. Predicted temporal concentration distributions in the fracture by low-order Padé approximation, high-order one and Tang et al.'s solution [1].

4. Concluding remarks

Four different approximate solutions for the problem of contaminant transport in a single fractured medium presented in Tang et al. [1] have been developed. The small-time and large-time solutions are derived based on the relationships of *LPST* and *SPLT*, respectively. The solutions with low-order and high-order approximations over the entire time domain are developed in accordance with the Padé approximation technique. These solutions can reduce to a very simple expression in terms of an exponential function and a complementary error function. We have investigated the accuracy of the present solutions by comparing with Tang et al.'s solution [1]. Following conclusions can be drawn in regard to the applicability and/or accuracy of the present solutions:

1. The predicted results indicate that the small-time solution provides an accurate approximation within a relatively small period of time while the large-time solution shows excellent agreement with the Tang et al.'s solution at late times.
2. The low-order Padé approximate solution gives excellent results in the intermediate and late periods. The predicted concentration by the high-order Padé approximation solution is slightly better than the low-order one, especially in the intermediate time.

3. It can be concluded that the Padé approximation solution has an advantage of being capable of producing more accurate results than the relationships of *SPLT* and *LPST* in the intermediate and late time periods.

Those results indicate that the present approximate solutions have the advantages of easy calculation and good accuracy from engineering viewpoint. They may be used as convenient tools to evaluate the temporal and spatial concentration distributions in performing risk assessment and site screening for industrial waste landfill and radioactive waste disposal.

Acknowledgment

This study was partially supported by the Taiwan National Science Council under Grant numbers NSC 99-2221-E-009-062-MY3 and NSC 101-2221-E-009-105-MY2.

References

[1] D.H. Tang, E.O. Frind, E.A. Sudicky, Contaminant transport in fractured porous media: analytical solution for a single fracture, Water Resour. Res. 17 (1981) 555–564.
[2] E.A. Sudicky, E.O. Frind, Contaminant transport in fractured porous media: analytical solutions for a system of parallel fractures, Water Resour. Res. 18 (1982) 1634–1642.
[3] E.A. Sudicky, E.O. Frind, Contaminant transport in fractured porous media: analytical solution for a two-member decay chain in a single fracture, Water Resour. Res. 20 (1984) 1021–1029.
[4] G.B. Davis, C.D. Johnston, Comment on "contaminant transport in fractured porous media: analytical solutions for a system of parallel fractures", Water Resour. Res. 20 (1984) 1321–1322.
[5] S.Y. Yang, H.D. Yeh, Laplace-domain solutions for radial two-zone flow equations under the conditions of constant-head and partially penetrating well, J. Hydraul. Eng. ASCE 131 (3) (2005) 209–216.
[6] H.D. Yeh, Y.C. Chang, Recent advances in modeling of well hydraulics, Adv. Water Resour. 51 (2013) 27–51.
[7] S.J. Farlow, Partial Differential Equations for Scientists and Engineers, Wiley, New York, 1982.
[8] D.K. Batu, M.T. Van Genuchten, A perturbation solution of the nonlinear Boussinesq equation: the case of constant injection into a radial aquifer, J. Hydrol. 48 (3–4) (1980) 269–280.
[9] K.N. Moutsopoulos, V.A. Tsihrintzis, Approximate analytical solutions of the Forchheimer equation, J. Hydrol. 309 (1–4) (2005) 93–103.
[10] R. Wallach, J.Y. Parlange, Modeling transport in a single crack by the dual-porosity concept with a boundary layer at the interface, J. Contam. Hydrol. 34 (1998) 121–138.
[11] H.D. Yeh, C.T. Wang, Large-time solutions for groundwater flow problems using the relationship of small *p* versus large *t*, Water Resour. Res. 43 (2007) W06502, http://dx.doi.org/10.1029/2006WR005472.
[12] M.G. Trefry, Analytical series expressions for Hantush's M and S functions, Water Resour. Res. 34 (4) (1998) 909–913.
[13] W.A. Illman, D.M. Tartakovsky, Asymptotic analysis of three-dimensional pressure interference tests: a point source solution, Water Resour. Res. 41 (1) (2005) W01002, http://dx.doi.org/10.1029/2004WR003431.
[14] J.E. Akin, J. Counts, On rational approximations to the inverse Laplace transform, SIAM J. Appl. Math. 17 (6) (1969) 1035–1040.
[15] I.M. Longman, Best rational function approximation for Laplace transform inversion, SIAM J. Math. Anal. 5 (4) (1974) 574–580.
[16] J.E. Heavilin, B.T. Neilson, Approximation of inverse Laplace transform solution to heat transport in a stream system, Water Resour. Res. 48 (2012) W09603, http://dx.doi.org/10.1029/2012WR012329.
[17] H.S. Carslaw, J.C. Jaeger, Conduction of Heat in Solids, second ed., Oxford University Press, New York, 1959, pp. 494–495.
[18] F. Oberhettinger, L. Badii, Tables of Laplace Transforms, Springer-Verlag, Heidelberg Berlin, New York, 1973, p. 264.
[19] C.F. Gerald, P.O. Wheatley, Applied Numerical Analysis, fifth ed., Addison-Wesley, 1994.
[20] D. Elliott, Truncation errors in Padé approximations to certain functions: an alternative approach, Math. Comput. 21 (99) (1967) 398–406.
[21] IMSL Fortran library user's guide math/library volume 2 of 2, visual numerics. Version 5.0, Houston, Texas, 2003.
[22] K.S. Crump, Numerical inversion of Laplace transforms using a Fourier series approximation, J. Assoc. Comput. Mach. 23 (1) (1976) 89–96.
[23] F.R. de Hoog, J.H. Knight, A.N. Stokes, An improved method for numerical inversion of Laplace transforms, SIAM J. Sci. Stat. Comput. 3 (3) (1982) 357–366.
[24] H.D. Yeh, S.Y. Yang, A novel analytical solution for constant-head test in a patchy aquifer, Int. J. Numer. Anal. Methods Geomech. 30 (12) (2006) 1213–1230.